JGR Oceans

RESEARCH ARTICLE
10.1029/2023JC020488

Key Points:

- We use D/L-amino acids to assess the bioreactivity and bacterial origins of particulate organic matter (POM) in the dynamic Changjiang Estuary and adjacent area
- High bioavailability of POM occurs in productive regions affected by Changjiang River plume, cyclonic eddies and typhoons
- Hot spots of bioavailable POM represent important sites for carbon sequestration

Supporting Information:

Supporting Information may be found in the online version of this article.

Correspondence to:

H. Yuan and J. Song,
yuanhuamao@qdio.ac.cn;
jmsong@qdio.ac.cn

Citation:

Guo, J., Zhou, B., Achterberg, E. P., Song, J., Duan, L., Li, X., & Yuan, H. (2024). Influence of hydrodynamics on the composition and reactivity of particulate organic matter in a large river influenced ocean margin. *Journal of Geophysical Research: Oceans*, *129*, e2023JC020488. https://doi.org/10.1029/2023JC020488

Received 14 SEP 2023
Accepted 6 JAN 2024

Influence of Hydrodynamics on the Composition and Reactivity of Particulate Organic Matter in a Large River Influenced Ocean Margin

Jinqiang Guo[1,2,3], Bu Zhou[1,3,4,5], Eric P. Achterberg[2], Jinming Song[1,3,4,5], Liqin Duan[1,3,4,5], Xuegang Li[1,3,4,5], and Huamao Yuan[1,3,4,5]

[1]Key Laboratory of Marine Ecology and Environmental Sciences, Institute of Oceanology, Chinese Academy of Sciences, Qingdao, China, [2]Marine Biogeochemistry Division, GEOMAR Helmholtz Centre for Ocean Research Kiel, Kiel, Germany, [3]University of Chinese Academy of Sciences, Beijing, China, [4]Laboratory for Marine Ecology and Environmental Sciences, Laoshan Laboratory, Qingdao, China, [5]Center for Ocean Mega-Science, Chinese Academy of Sciences, Qingdao, China

Abstract Marginal seas influenced by large rivers are characterized by complex hydrodynamic and organic matter cycling processes. However, the impacts of hydrodynamics on the composition and reactivity of particulate organic matter (POM) remain unclear. Here we conducted a comprehensive study on the bulk, molecular and biological properties of suspended POM in the Changjiang Estuary and adjacent area subjected to strong currents, eddies as well as typhoons during spring and autumn. D/L-enantiomers of particulate amino acids (PAA) were analyzed to evaluate the bioreactivity of POM and quantify bacterial-derived organic carbon. We found that POM bioavailability as indicated by carbon-normalized yields of PAA (PAA-C%) reflected the ecosystem productivity. Relatively high PAA-C% values (20−35%) were observed in productive areas influenced by Changjiang River plume, cyclonic eddies and typhoons, likely related to the enhanced nutrient availability arising from hydrodynamic processes. In contrast, the oligotrophic Taiwan Warm Current-influenced regions featured relatively low POM bioavailability (PAA-C% < 10%) despite typhoons facilitating water mixing. The PAA-C% values showed a significant positive correlation with extracellular enzyme activity, indicating that bioavailable POM can rapidly stimulate heterotrophic transformation. Hot spots of elevated bioavailable POM showed high contributions of bacterial organic carbon. A large portion (~2/3) of bacterial organic carbon was present in the form of bacterial detritus, suggesting that patches of these biological hot spots represent important sites of carbon sequestration. Together, our findings indicate that fresh POM production is largely controlled by nutrient supply driven by hydrodynamic processes, with important implications for carbon sequestration in the dynamic ocean margins.

Plain Language Summary Marginal seas are subject to complex hydrodynamic processes and play an important role in carbon sequestration. Disentangling the linkages between hydrodynamics and organic carbon reactivity and composition is crucial to understanding the regional carbon cycle. Here we collected suspended particulate organic matter (POM) in the Changjiang Estuary and adjacent coastal areas. Based on the biomarker D/L-amino acids, we assessed the bioavailability of POM and quantified the organic carbon originating from bacteria. We found that high bioactivity of POM occurred in productive Changjiang River plume, cyclonic eddy, and typhoon influenced areas. These hydrodynamic processes appear to increase nutrient availability, therefore promoting phytoplankton growth. Bioavailable POM can rapidly stimulate heterotrophic activity and facilitate the transformation of algal-derived organic carbon to bacterial detritus, thus contributing to carbon sequestration. Our findings suggest that the production of bioavailable POM is largely controlled by hydrodynamically driven nutrient supply.

1. Introduction

Marginal seas cover ~7% of the global ocean surface area but are characterized by high primary productivity, active heterotrophic metabolism and rapid organic carbon burial, playing an important role in the global carbon cycle (Andersson & Mackenzie, 2004; Bauer et al., 2013; Burdige, 2005; Canuel & Hardison, 2016; Gattuso et al., 1998). Organic matter from autotrophic and heterotrophic sources is subject to dynamic processes in coastal systems, and the impacts of human activities and climate change are superimposed on these processes, making marginal seas complex hot spots for carbon sequestration and air-sea exchange of carbon dioxide (CO_2) (Bauer

et al., 2013; Dai et al., 2022). Over the past decades, this topic has attracted extensive attention, yet the role of marginal seas as a carbon source or sink remains under debate (Borges et al., 2005; Cai, 2011; Dai et al., 2013, 2022).

Marginal seas are characterized by complex hydrodynamic processes that are tightly linked to organic matter cycling (Bao et al., 2018; Chen et al., 2021; Guo et al., 2018; Liu et al., 2019; Pedrosa-Pamies et al., 2013). In particular, on ocean margins influenced by large rivers, the convergence of plumes with ocean currents generates a series of fronts and exerts a pronounced impact on phytoplankton production and the development of hypoxia in bottom waters (Guo et al., 2020; Lv et al., 2022; Wei et al., 2021). Ocean currents with different physical and chemical (e.g., nutrient) characteristics feature divergent primary production (Chen, 2009; Zhang et al., 2007). Coastal currents are typically enriched in nutrients due to terrestrial inputs and have enhanced primary productivity (Chen, 2009; Guo et al., 2018). In addition, marginal seas are subject to eddies and typhoons. Cyclonic eddies and typhoons can stimulate phytoplankton production by transferring nutrients from deeper waters to the surface layer (Li et al., 2019; Shih et al., 2020; Siswanto et al., 2009). The organic matter derived from phytoplankton production is typically bioavailable and fuels bacterial respiration and growth (Amon & Benner, 1998; Obernosterer et al., 2008). Fresh particulate organic matter (POM) typically contains relatively high fractions of carbohydrates and amino acids (Li et al., 2018; Unger et al., 2005), thus facilitating attached bacterial proliferation coupled with increased extracellular enzyme activity (EEA) (Herndl & Reinthaler, 2013; Zhou et al., 2021). Regions with high concentrations of bioavailable POM therefore represent biological hot spots where rapid heterotrophic transformation and elemental cycling occur (Guo, Shen et al., 2023; Shen et al., 2016; Stocker et al., 2008).

Investigating POM composition and bioavailability under different physical forcings in ocean margins will improve our understanding of the regional carbon cycle. Prior studies have indicated that the composition of organic matter varies between water masses (Chen et al., 2021; Guo et al., 2018). However, it remains challenging to determine the influence of hydrodynamics on organic matter transformation and reactivity in dynamic marginal seas at large spatiotemporal scales.

Biomarkers provide powerful tools for tracing bioavailable organic matter. Amino acids are bioactive organic molecules and are preferentially removed during the degradation of organic matter (Amon et al., 2001; Cowie & Hedges, 1994; Davis et al., 2009). The carbon- and nitrogen-normalized yields of amino acids have been used as indicators of organic matter bioavailability over a wide range of spatial and temporal scales in different aquatic systems (Davis & Benner, 2005; Guo, Zhou, et al., 2023; Kaiser & Benner, 2012; Liang et al., 2023; Shen et al., 2017). Amino acid composition also provides insights into the extent of organic matter alteration. Based on the variations in amino acid molar composition during early diagenesis, Dauwe et al. (1999) proposed a degradation index (DI) as a reliable proxy reflecting the degradation history of organic matter. In addition, microorganisms can leave molecular imprints, such as D-enantiomers of amino acids (D-AA), during organic matter diagenetic alterations (Lehmann et al., 2020; McCarthy et al., 1998). D-AA are important components of bacterial cell wall peptidoglycans and are useful biomarkers to estimate bacterial contributions to marine organic matter (Guo, Zhou, et al., 2023; Kaiser & Benner, 2008).

In this study, a comprehensive data set is examined on particulate organic carbon (POC), D/L-amino acids, nutrients, EEA (for leucine aminopeptidase), bacterial abundance and community structure during spring and autumn in the dynamic Changjiang Estuary and adjacent area (CEAA). Hydrological parameters are used to indicate the effects of water masses, eddies, and typhoons. Our primary objective is to investigate the hydrodynamic and biological controls on POM distribution and chemical composition, with a particular emphasis on the diagenetic state of POM. Furthermore, the implications of hydrodynamically driven biological hot spots for carbon sequestration are discussed.

2. Materials and Methods

2.1. Hydrography and Sampling

The study region includes the Changjiang Estuary and adjacent South Yellow Sea and East China Sea (Figure 1), and is characterized by a complex circulation of water masses (Chen, 2009). Diverse currents converge in the East China Sea, including the Changjiang Diluted Water (CDW), Taiwan Warm Current (TWC), and Kuroshio Current (KC). The CDW originates in the Changjiang River and the edge of its plume expansion is typically marked by a

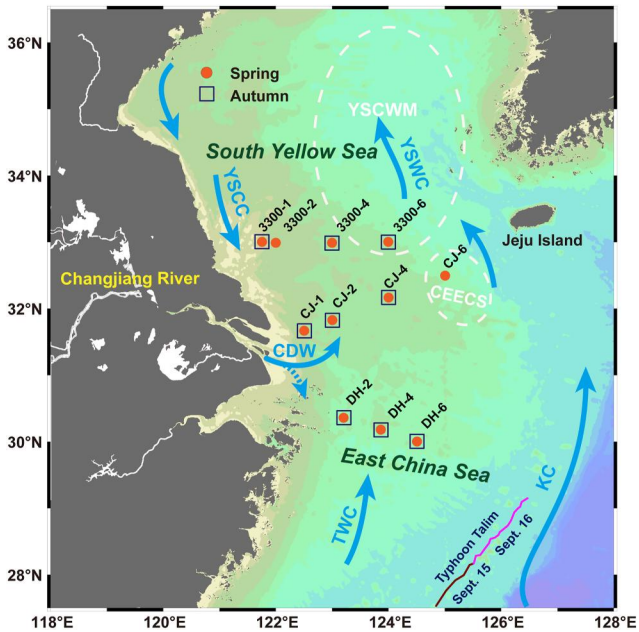

Figure 1. Sampling regions in the South Yellow Sea and East China Sea during spring (April 25−May 2) and autumn (September 7−September 24) of 2017. Brown and pink lines represent the track of Typhoon Talim (typhoon data from website: http://typhoon.weather.com.cn/); Shelf circulations are labeled as follows: CDW, Changjiang Diluted Water; CEECS, Cold Eddy in the East China Sea; KC, Kuroshio Current; TWC, Taiwan Warm Current; YSCC, Yellow Sea Coastal Current; YSCWM, Yellow Sea Cold Water Mass; YSWC, Yellow Sea Warm Current.

salinity 31. The mainstream of the strong western boundary KC flows northeastward along the continental shelf break, whereas its TWC branch flows northward through the Taiwan Strait (Yang et al., 2011). In summer, the frontal water of the TWC can intrude into the shallow waters of the northeastern Changjiang Estuary (Wei et al., 2021). The South Yellow Sea is influenced by the southward Yellow Sea Coastal Current (YSCC), the northward Yellow Sea Warm Current (YSWC), and the Yellow Sea Cold Water Mass (YSCWM) in the central South Yellow Sea. Physical interactions between the water masses create eddies in the South Yellow Sea and East China Sea (Hu & Wang, 2016; Lan et al., 2010; Shi et al., 2016). The East China Sea is also influenced by frequent typhoon activity during summer and autumn.

Samples were collected within the 100 m isobath on the continental shelf aboard R/V *Kexue* 3 during spring (April 25−May 2) and autumn (September 7−September 24) of 2017 (Figure 1). Sample collection along the Changjiang (CJ) and Donghai (DH) sections in autumn occurred after the passage of Typhoon Talim (September 15−September 16). Water samples were collected at discrete depths (2, 5, 10, 20, 30 m and bottom layer) using a rosette sampler system fitted with 12 L Niskin bottles. In situ temperature and salinity were determined by Conductivity-Temperature-Depth (CTD; Seabird) sensors. Samples for dissolved oxygen (DO) were collected in 100 mL brown glass bottles. Samples for analyses of POC, particulate nitrogen (PN) and particulate amino acids (PAA) were filtered over pre-combusted (450°C, 5 hr) glass fiber filters (GF/F, 0.7 μm pore size, Whatman) and stored frozen (−20°C). The filtrate was collected in acid-cleaned 60 mL high-density polyethylene (HDPE) bottles and stored at −20°C for further analysis of inorganic nutrients. Filtered (0.7 μm pore size GF/F filters) and unfiltered water samples (4 mL) were collected and immediately fixed with paraformaldehyde (final concentration: 1%) and stored in liquid nitrogen for heterotrophic bacterial abundance (HBA) analysis. Samples for EAA and bacterial community analyses were filtered onto pre-combusted (450°C, 5 hr) GF/F filters (0.7 μm pore size, Whatman) and stored at −80°C. Detailed analysis information of EAA and bacterial community is provided in Text S1 and S2 in Supporting Information S1. Samples for chlorophyll-*a* (Chl-*a*) measurements were collected using cellulose acetate membranes and stored frozen (−20°C) in the dark until analysis.

2.2. Chemical and Biological Analyses

2.2.1. Chlorophyll-*a*, Dissolved Oxygen and Nutrients

The filters for Chl-*a* determination were extracted with 10 mL 90% acetone at 4°C for 24 hr, centrifuged, and analyzed using a Hitachi F-4,600 fluorescence spectrophotometer (excitation: 436 nm; emission: 670 nm). Concentrations of DO were determined immediately after collection onboard by a Seven Excellence DO meter S900 equipped with an optical probe (Mettler-Toledo International Inc.). Winkler titrations (Bryan et al., 1976) were performed to calibrate the DO probe. Concentrations of nitrate (NO_3-N), nitrite (NO_2-N), ammonium (NH_4-N) and phosphate (PO_4-P) were analyzed using a Bran-Lubbe Quaatro-SFA autoanalyzer (Guo et al., 2020). The dissolved inorganic nitrogen (DIN) was the sum of NO_3-N, NO_2-N and NH_4-N.

2.2.2. Particulate Organic Carbon and Particulate Nitrogen

Samples for POC and PN determination were fumigated with hydrochloric acid (HCl) to remove inorganic carbonate, oven-dried at 60°C, and analyzed using a Flash EA IsoLink CN elemental analyzer (Thermo Fisher Scientific, Germany).

2.2.3. Particulate Amino Acids

Filters for amino acids analysis were hydrolyzed in sealed ampoules with 6 mol L^{-1} HCl at 110°C for 24 hr after being freeze-dried. Following hydrolysis, the HCl was removed by repeated drying under nitrogen gas and the

sample re-dissolved with 0.002 mmol L^{-1} HCl (adjusted to pH = 8.5). Amino acid enantiomers were derivatized with *o*-phthaldialdehyde (OPA) and N-isobutyryl-L-cysteine (IBLC) and were separated by high-performance liquid chromatography/fluorescence detection (excitation: 300 nm; emission: 445 nm) system equipped with a SunFireTM RPC18 column (4.6 × 250 mm, 5 μm particles) (Fitznar et al., 1999). Sixteen amino acids were included in the analysis: asparagine + aspartic acid (Asx), glutamine + glutamic acid (Glx), serine (Ser), histidine (His), glycine (Gly), threonine (Thr), arginine (Arg), alanine (Ala), tyrosine (Tyr), valine (Val), phenylalanine (Phe), isoleucine (Ile), leucine (Leu), and lysine (Lys). Racemization induced by acid hydrolysis was corrected according to Kaiser and Benner (2005).

The carbon- and nitrogen-normalized yields of PAA were calculated as follows:

$$\text{PAA-C\%(orPAA-N\%)} = \frac{\text{PAA-C(orN)}}{\text{POC (or PN)}} \times 100 \quad (1)$$

where POC (or PN) and PAA-C (or N) are the concentrations of bulk POC (or PN) and carbon (or nitrogen) measured in the total PAA, respectively.

The DI was calculated based on principal component analysis (PCA) and the mole percentage of amino acids as shown in Equation 2:

$$\text{DI} = \sum_i \left[\frac{\text{var}_i\text{-AVG var}_i}{\text{STD var}_i} \right] \times \text{fac.coef}_i \quad (2)$$

where var_i is the mole percentage of amino acid *i*, AVG var_i and STD var_i are the mean and standard deviation of the mole percentage of amino acid *i*, and fac. coef_i is the factor coefficient for amino acid *i* in the first axis of the PCA (Dauwe et al., 1999).

Bacterial contributions to POC were determined following the method of Kaiser and Benner (2008):

$$\text{Bacterial OC (\%)} = \frac{\text{Biomarker}_{\text{OC}}}{\text{Biomarker}_{\text{Bacteria}}} \times 100 \quad (3)$$

where $\text{Biomarker}_{\text{OC}}$ and $\text{Biomarker}_{\text{Bacteria}}$ are the carbon-normalized yields of D-Ala in POC and bacteria, respectively. The $\text{Biomarker}_{\text{Bacteria}}$ yields used in the calculations were 78.7 nmol mg C^{-1} and 81.8 nmol mg C^{-1} based on the average bacterial composition of the study area in spring (78% Gram-negative heterotrophs, 14% Gram-negative phototrophs and 8% Gram-positive heterotrophs) and autumn (68% Gram-negative heterotrophs, 22% Gram-negative phototrophs and 10% Gram-positive heterotrophs), respectively (Figure S1 in Supporting Information S1). D-Ala yields in marine Gram-negative heterotrophic bacteria, Gram-negative phototrophic bacteria and Gram-positive heterotrophic bacteria were 58.9, 16.0 and 381.9 nmol mg C^{-1}, respectively (Kaiser & Benner, 2008).

2.2.4. Heterotrophic Bacterial Cell Counts

Abundances of heterotrophic bacteria were determined by flow cytometry as described by Zhao et al. (2011). Briefly, seawater samples were diluted five times with Tris-EDTA buffer and stained with the nucleic acid dye SYBR Green I (Molecular Probes). Total bacterial counts were determined in unfiltered seawater samples, and free-living bacteria (<0.7 μm) were counted in filtered samples. The particle-attached bacterial abundance (>0.7 μm) was estimated by subtracting the free-living bacteria from the total bacterial counts.

3. Results

3.1. Hydrography and Biogeochemical Variables

In spring, temperature and salinity ranged from 10.8°C to 17.9°C (average: 14.0 ± 2.0°C) and 26.6 to 34.2 (average: 31.9 ± 1.5), respectively (Figure 2). Generally, the surface water temperature increased from north to south and from nearshore to offshore along the three sections. An obvious water tongue of low salinity and enhanced temperature existed in the nearshore surface waters of the CJ section (Figure 2). In contrast, relatively

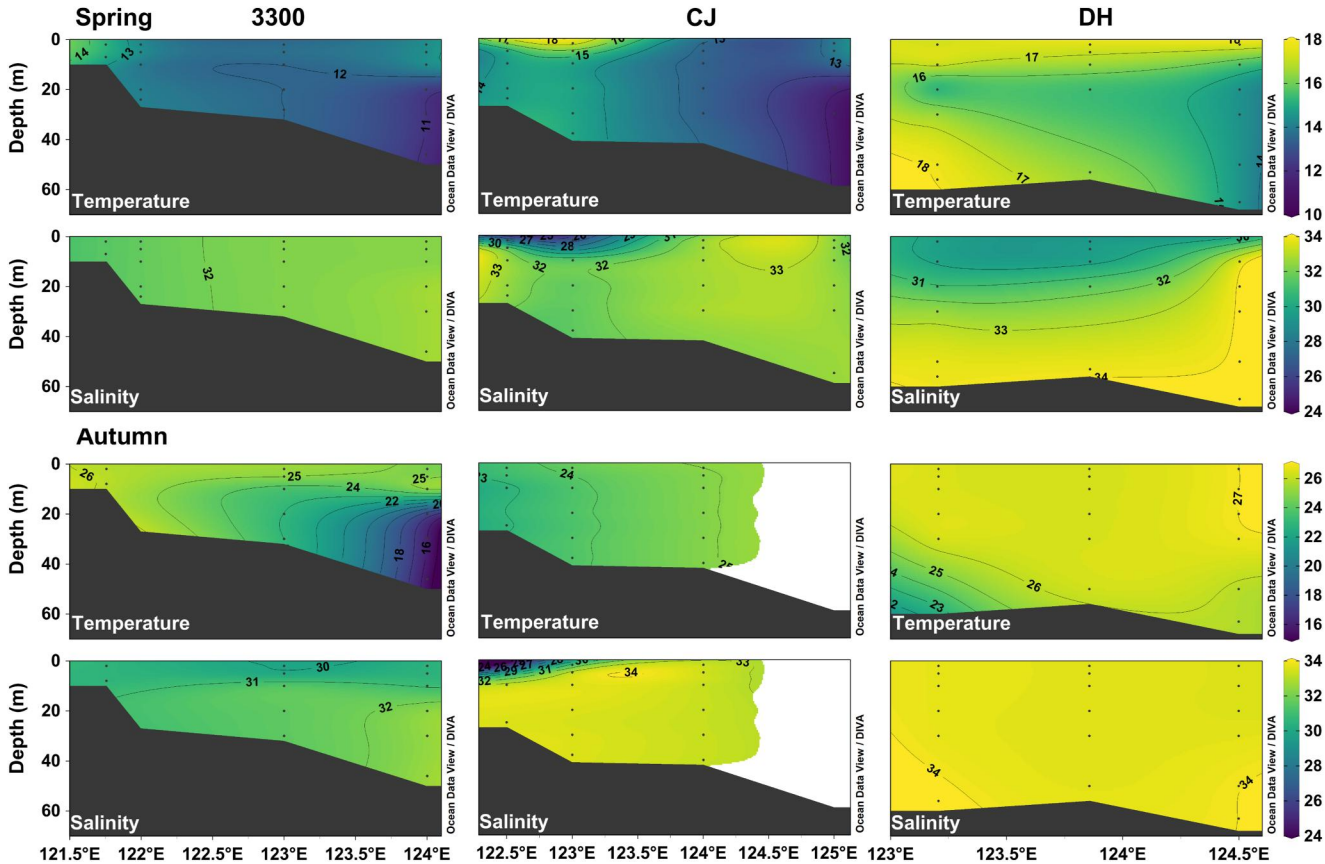

Figure 2. Sections of temperature and salinity for transects 3300, CJ and DH during spring and autumn.

low temperatures and high salinities were found at the offshore stations 3300-6 and CJ-6 below 20 m water depth (Figure 2). The highest salinity (34.1) was observed in offshore subsurface waters of the TWC-influenced DH section (Figure 2). In autumn, the temperature ranged from 15.5°C to 27.0°C with an average of 24.6 ± 2.5°C. Elevated temperatures were observed in nearshore surface waters of transect 3300 and in the offshore region of transect CJ (Figure 2). Salinity ranged from 24.6 to 34.2 (average: 32.6 ± 1.8), with the lowest values in the surface water of station CJ-1. Similar to the spring, low temperature and high salinity were observed below the thermocline (>20 m) at station 3300-6. Following Typhoon Talim, the vertical distributions of temperature and salinity in CJ and DH sections were essentially uniform, especially in the offshore areas (Figure 2).

Concentrations of Chl-*a* ranged from 0.7 to 5.6 μg L^{-1} (mean: 1.9 ± 1.3 μg L^{-1}) in the spring (Figure 3). High values were found in nearshore surface waters along transects CJ and DH. In comparison, Chl-*a* concentrations ranged from 0.1 to 12.6 μg L^{-1} (mean: 2.7 ± 3.5 μg L^{-1}) in autumn and reached significantly higher values than in spring (Mann-Whitney *U* Test, $p < 0.05$). At station CJ-4, the water column displayed high Chl-*a* concentrations (>8 μg L^{-1}). Concentrations of Chl-*a* were distributed relatively uniformly throughout the water column along transect DH and were much lower than those along the CJ and 3300 transects (Figure 3). Concentrations of DO ranged from 6.5 to 9.7 mg L^{-1} and 1.7 and 7.5 mg L^{-1} in spring and autumn, respectively. Distributions of DO showed similar patterns to Chl-*a*, except for waters below 10 m at station 3300-4 in autumn (Figure 3).

Generally, concentrations of DIN in spring exhibited a decreasing trend in an offshore direction (Figure 3). In contrast, PO_4-P distributions were considerably variable. Relatively low values of PO_4-P were observed in the offshore regions of section 3300, while high PO_4-P concentrations were found in the bottom layers of section DH (Figure 3). In autumn, depleted nutrients were found in offshore regions of transects 3300 and CJ (Figure 3). Nutrient concentrations were low and vertically distributed uniformly in the DH section in autumn (Figure 3).

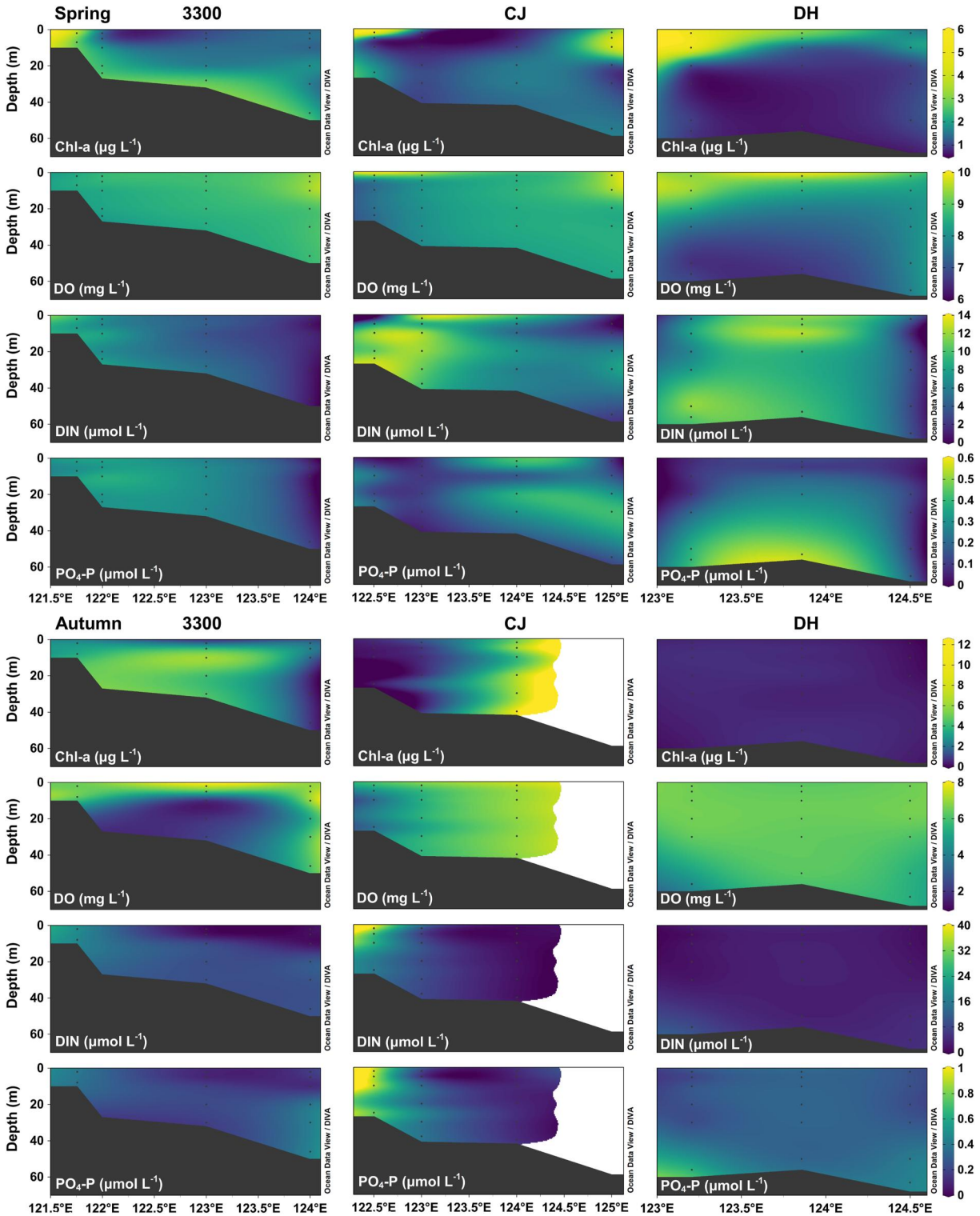

Figure 3. Sections of chlorophyll-*a* (Chl-*a*), dissolved oxygen (DO), dissolved inorganic nitrogen and phosphate (PO_4-P) for transects 3300, CJ and DH in the Changjiang Estuary and adjacent area during spring and autumn.

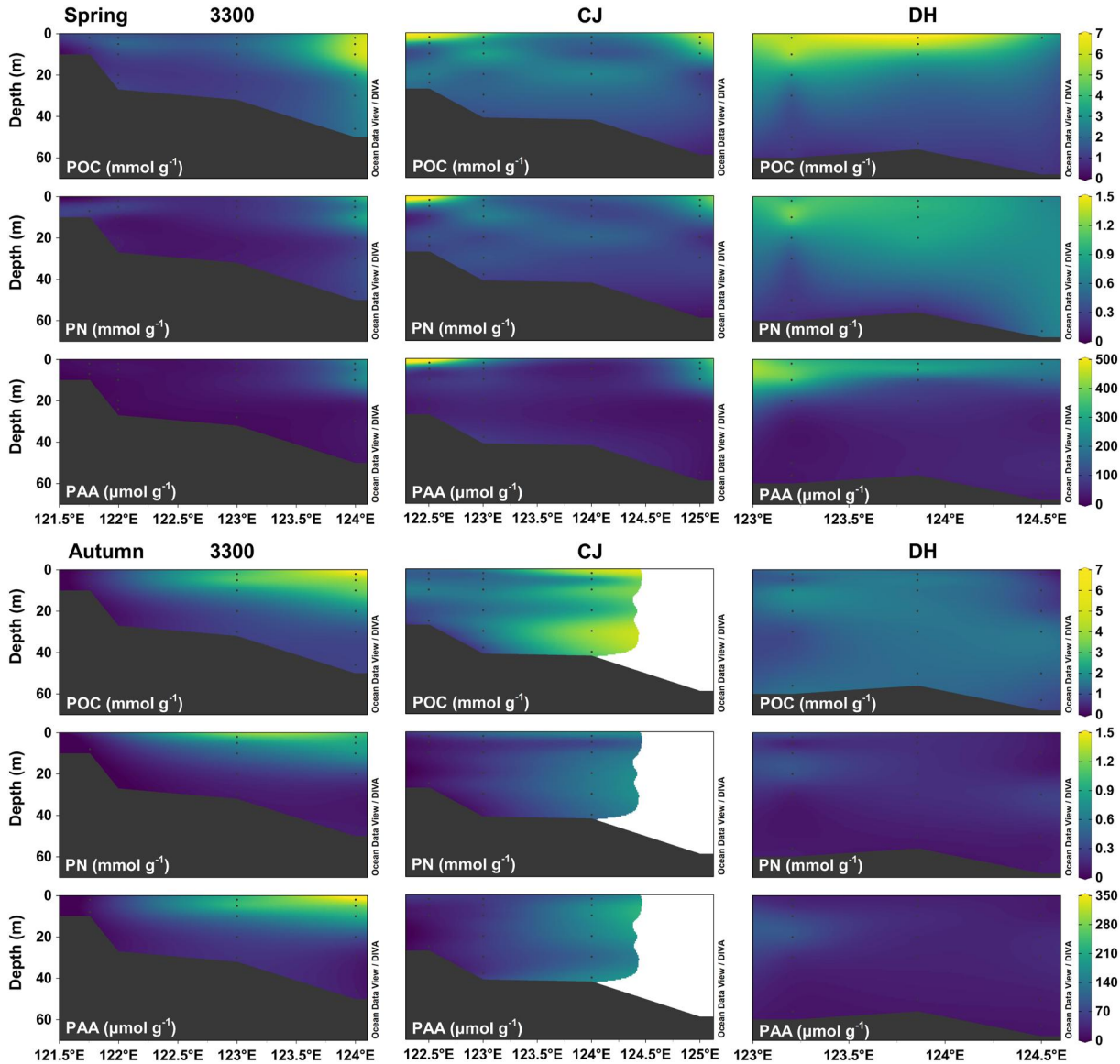

Figure 4. Sections of particulate organic carbon (POC), particulate nitrogen (PN) and particulate amino acids (PAA) in the Changjiang Estuary and adjacent area during spring and autumn.

3.2. Distributions and Characteristics of POM

In the study region, concentrations of POC and PN during spring varied from 0.50 mmol g^{-1} to 6.81 mmol g^{-1} (average: 2.30 ± 1.69 mmol g^{-1}) and 0.09 mmol g^{-1} to 1.46 mmol g^{-1} (mean: 0.45 ± 0.33 mmol g^{-1}), respectively (Figure 4). Patches with markedly higher POC and PN concentrations were observed in upper waters (<20 m). Comparable POC and PN concentrations were observed in autumn, ranging from 0.50 mmol g^{-1} to 6.75 mmol g^{-1} (average: 2.08 ± 1.45 mmol g^{-1}) and from 0.04 mmol g^{-1} to 1.13 mmol g^{-1} (average: 0.31 ± 0.26 mmol g^{-1}), respectively (Figure 4). In autumn, elevated POC and PN concentrations were mostly observed in offshore upper waters along transect 3300 and the entire water column of station CJ-4 (Figure 4).

Concentrations of PAA were quite variable in spring, ranging by ~60-fold from 8.1 to 461.9 μmol g^{-1} (average: 98.4 ± 107.8 μmol g^{-1}), while PAA varied between 12.3 and 349.0 μmol g^{-1} with an average of 79.5 ± 79.1 μmol g^{-1} in autumn (Figure 4). There was no significant difference in PAA concentrations between spring and autumn (Mann-Whitney U Test, $p > 0.05$). In general, PAA exhibited similar distribution patterns to POC and PN.

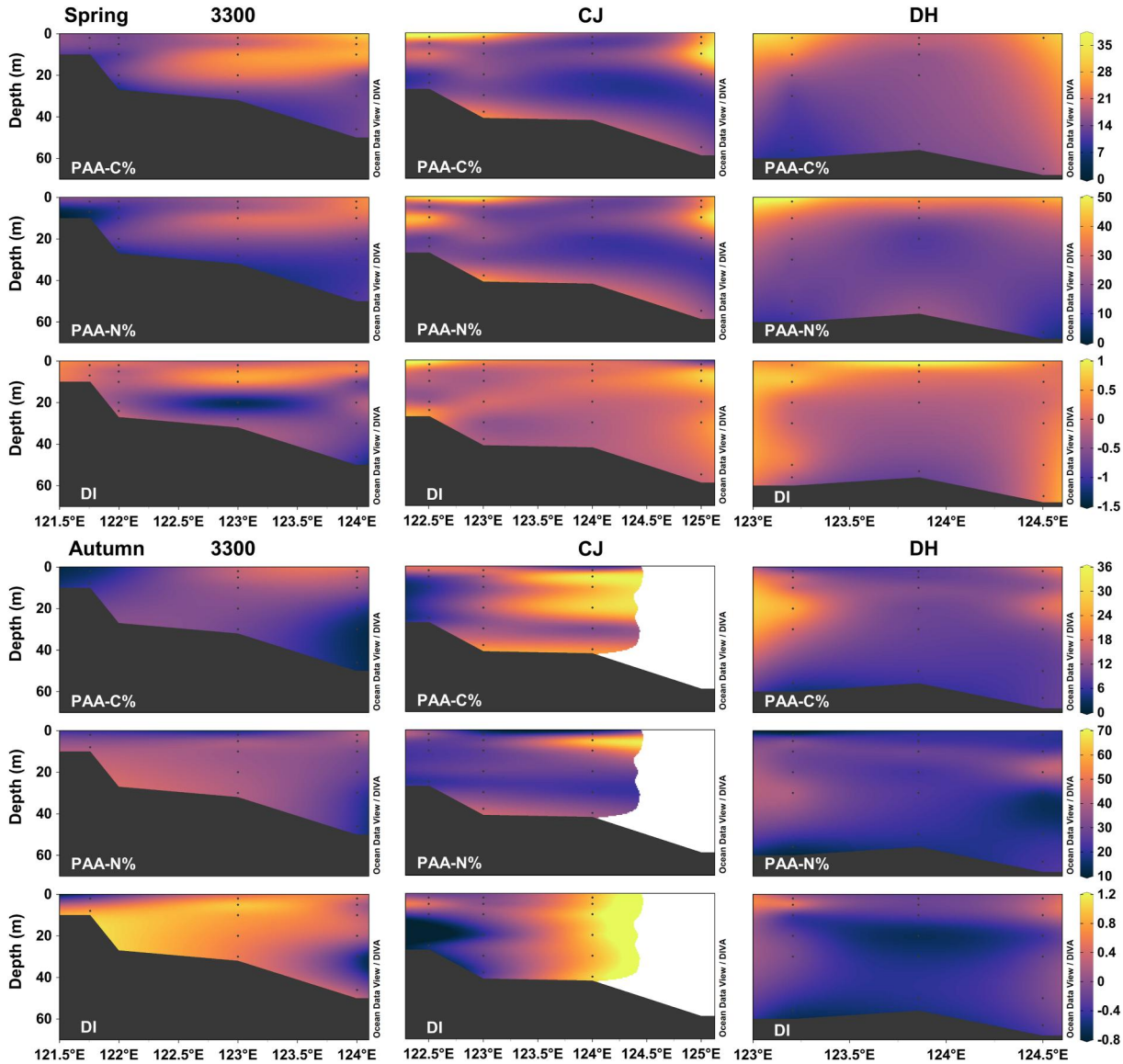

Figure 5. Sections of carbon-normalized yields of particulate amino acids (PAA) (PAA-C%), nitrogen-normalized yields of PAA (PAA-N%) and degradation index (DI) in the Changjiang Estuary and adjacent area during spring and autumn.

3.3. Degradation Indicators

In spring, PAA-C% and PAA-N% values displayed considerable variability, ranging from 4.9% to 37.2% (mean: 15.6 ± 8.0%) and 4.1%–48.9% (mean: 21.9 ± 11.3%), respectively (Figure 5). Vertical distributions of PAA-C% and PAA-N% were similar to those of POC, with high values (PAA-C%: >25%; PAA-N%: >30%) occurring in both nearshore and offshore upper waters of the CJ and DH sections, as well as above 20 m offshore along section 3300 (Figure 5). Values of PAA-C% and PAA-N% were also highly variable in autumn and ranged from 5.5% to 36.1% (mean: 15.1 ± 6.7%) and 14.2%–66.7% (mean: 29.3 ± 10.0%), respectively. Remarkable increases in PAA-C% were observed in the offshore upper layers of transects 3300 and throughout the water column at station CJ-4 (Figure 5).

In the sampling region, DI varied from −1.40 to 0.93 (mean: −0.02 ± 0.43) in spring, and from −0.7 to 1.1 (mean: 0.59 ± 0.46) in autumn (Figure 5). Compared with sections 3300 and CJ, the vertical profiles of PAA-C%, PAA-N%, and DI were nearly homogeneous along section DH during autumn (Figure 5). Generally, DI and PAA-C% presented similar distribution trends for both seasons.

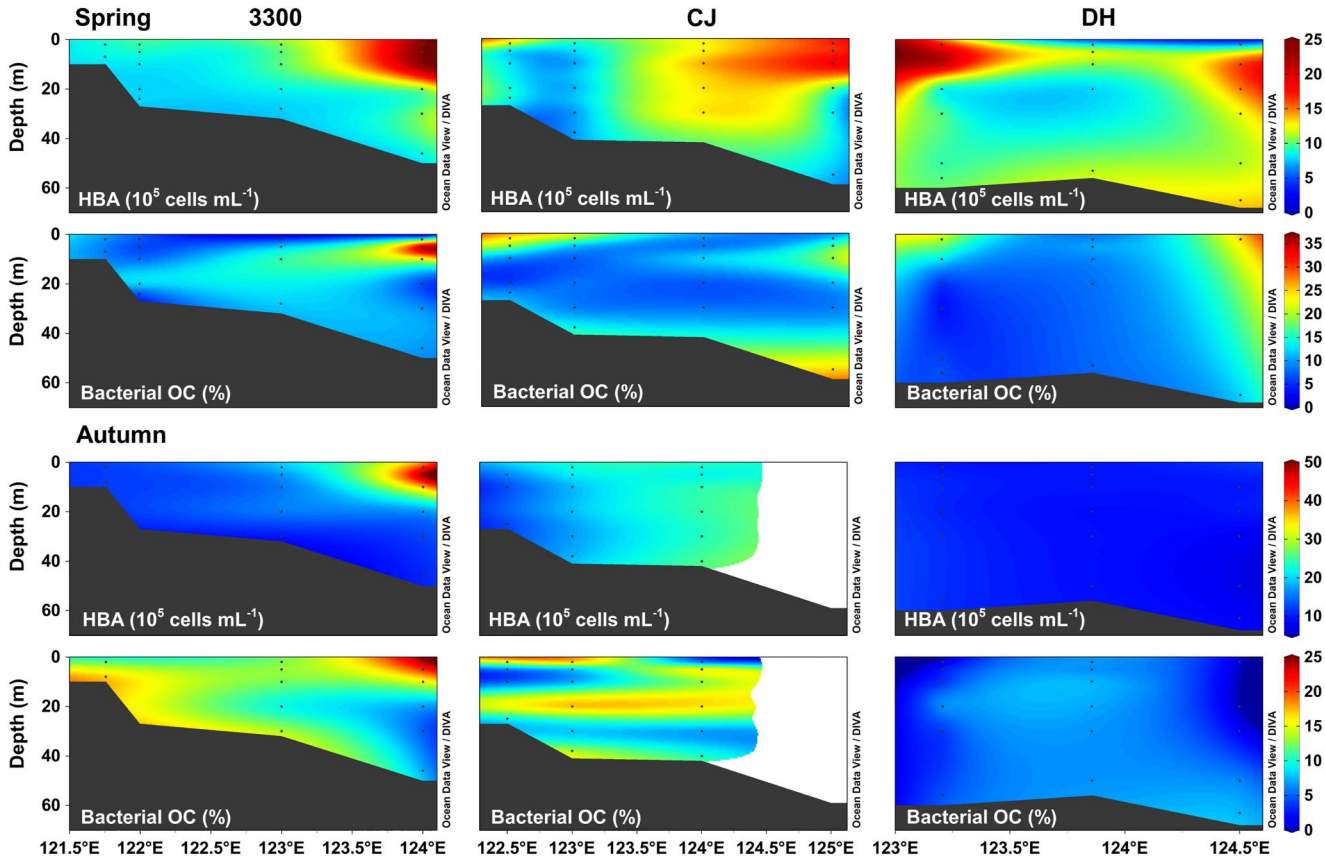

Figure 6. Sections of heterotrophic bacterial abundance (HBA) and bacterial contributions to particulate organic carbon (POC) in the Changjiang Estuary and adjacent area during spring and autumn.

3.4. Heterotrophic Bacterial Abundance and Bacterial Contributions to POC

Values of HBA varied from 4.8 to 24.9 × 10^5 cells mL^{-1} (mean: 10.2 ± 4.9 × 10^9 cells L^{-1}) in spring (Figure 6), and from 7.1 to 49.8 × 10^5 cells mL^{-1} (mean: 1.63 ± 0.89 × 10^9 cells L^{-1}) in autumn. The HBA was significantly higher in autumn than in spring (Mann-Whitney U Test, $p < 0.01$). A relatively high HBA was observed in offshore upper layers along transects 3300 and CJ, while elevated HBA occurred in both nearshore and offshore upper waters of transect DH. Similar to Chl-*a*, markedly high HBA appeared in the entire water column of station CJ-4 (Figure 6). In general, distributions of HBA in spring and autumn agreed with trends of PAA-C% and DI.

Bacterial contributions to POC ranged from 2.5% to 36.5% (mean: 11.9 ± 6.5%) in spring (Figure 6). Consistent with HBA, elevated bacterial OC (%) was found in offshore upper waters of transects 3300 and CJ. In contrast, bacterial contributions were vertically distributed evenly along transect DH, except for high values in the nearshore and offshore upper waters (Figure 6). During autumn, bacterial OC (%) varied from 0.3% to 24.0% (mean: 9.2 ± 5.6%) and was significantly lower than in spring (Mann-Whitney U Test, $p < 0.01$). The high bacterial contributions (>20%) found along section 3300 coincided with a high HBA. Unlike sections 3300 and CJ, the contributions of bacteria to POC were lower and less variable along section DH (Figure 6).

4. Discussion

4.1. Hydrodynamic Processes in the Study Region

Temperature and salinity allowed us to assess the hydrodynamics in the CEAA. Relatively low salinity was observed in the coastal surface layer of transects CJ and DH (Figure 2), indicating the influence of CDW. Driven by the East Asian monsoon, the CDW flows northeast in summer but southeast in winter (Chang & Isobe, 2003; Isobe et al., 2002). The average annual discharge of the Changjiang River for the period 2012−2021 was 93.97 × 10^{10} m^3 (http://www.cjh.com.cn/). Large nutrient loads into the Changjiang Estuary

result in frequent outbreaks of algal blooms and bottom hypoxia (Li et al., 2014; Zhu et al., 2011). The nearshore region of the 3300 section is subject to the southward YSCC with relatively low salinity (Figure 2). The YSCC receives terrestrial inputs and also features high nutrient concentrations (DIN >7 μmol L^{-1}; PO_4-P > 0.3 μmol L^{-1}). As a branch of the KC, the high-temperature, high-salinity but relatively oligotrophic (especially PO_4-P, ~0.2 μmol L^{-1}) TWC flows northward (Guo et al., 2018), exerting a profound impact on the biogeochemistry of the offshore region of the DH section. At the offshore sites of transect 3300, the thermocline was present at ~20 m (Figure 2). Previous studies have confirmed the low-temperature and high-salinity YSCWM below the subsurface layer in the central South Yellow Sea (Guo et al., 2020; Wang et al., 2014). The YSCWM is formed by the subduction of cold surface waters in winter (Lee & Beardsley, 1999) and forms an important nutrient reservoir, where DIN and PO_4-P stocks can account for 30.8% and 52.1% of the entire South Yellow Sea in autumn (Guo et al., 2020). Physical interactions between YSWC and YSCWM stimulate a cyclonic eddy in the central South Yellow Sea approximately along the 25 m isobath (Shi et al., 2016). Thermal structure and circulation data have confirmed the perennial presence of another cyclonic eddy located 150 km southwest of Cheju Island in the East China Sea, with a horizontal extent of 100–200 km and a vertical extent of 50 m (Lan et al., 2010). The uplift of temperature contours observed in the offshore regions of sections CJ and 3300 indicates the presence of cyclonic eddies (Figure 2). These two eddies could enhance primary production in the offshore regions of transects 3300 and CJ by upwelling nutrient-rich bottom waters.

Compared with spring, the vertical distributions of temperature and salinity were more uniform along the CJ and DH sections in autumn (Figure 2), which is likely related to the impact of Typhoon Talim. The sampling of the CJ and DH transects was conducted after the typhoon. During typhoons, the kinetic energy of the typhoon is transferred to the water column, resulting in strong vertical mixing.

4.2. Influence of Hydrodynamics on POM Distribution and Reactivity

Phytoplankton production exerts an important control on POM concentrations in the CEAA, as evidenced by the significant positive correlation between POC and Chl-*a* (spring: $r = 0.549$, $p < 0.01$; autumn: $r = 0.476$, $p < 0.01$). Amino acid composition provides insights into the phytoplankton origin of POM. Dittmar et al. (2001) found that the mol% Ser + Thr (diatomaceous POM: 16.9%; calcareous POM: 9.0%) and Asp/Gly ratio (diatomaceous POM: 0.62; calcareous POM: 1.88) could be used to identify diatomaceous and calcareous sources of POM. In the CEAA, the average mol% Ser + Thr and Asp/Gly ratios were 15.93 ± 0.87% and 0.81 ± 0.14 in spring, compared to 16.17 ± 0.73% and 0.81 ± 0.17 in autumn. These results indicate that diatoms were important sources of POM, consistent with the predominance of diatoms in the CEAA phytoplankton community (Guo et al., 2014).

Changes in POM bioavailability observed in the CEAA likely reflect variability in ecosystem productivity. In the present study, two degradation indicators established on the basis of amino acids were used to evaluate POM reactivity. In general, PAA-C% and DI have a good relationship in the CEAA ($r = 0.50$, $p < 0.01$). However, no single index can represent the full continuum of organic matter diagenesis. Davis et al. (2009) suggested that carbon-normalized amino acid yields are good indicators of early diagenesis, while DI is more sensitive during the intermediate stages of organic matter degradation. In the shallow marginal seas, the turnover time of POM is around days to weeks (Zhu et al., 2006), suggesting that PAA-C% is more reliable in indicating POM reactivity. Higher values of PAA-C% (20−35%) occurred in regions influenced by cyclonic eddies, CDW and the typhoon. Prior work has demonstrated that POM from the Changjiang River is recalcitrant and is rapidly removed in low-salinity areas (Liang et al., 2023; Wu et al., 2007). The salinity in our study area was >24, suggesting that the impact of terrestrial POM is likely small. In addition, significant positive correlations were found between PAA-C% and Chl-*a* (spring: $r = 0.38$, $p < 0.01$; autumn: $r = 0.56$, $p < 0.01$). These results indicate that bioavailable POM in the CEAA is linked to hydrodynamically regulated primary production. Cyclonic eddies can transfer nutrients from subsurface to upper waters, thereby stimulating primary production. Depleted nutrients were found in the offshore surface waters along transects 3300 and CJ (Figure 3), suggesting rapid consumption of nutrients by phytoplankton growth. Eddy-induced enhancement of primary production is further supported by the markedly elevated Chl-*a* concentrations in the offshore surface waters along section CJ (Figure 3). The CDW-influenced regions (e.g., the nearshore surface layer of section CJ) showed relatively high POM bioavailability in spring. As indicated by the distribution of salinity, the nearshore area of section CJ was more

strongly influenced by the nutrient-rich Changjiang River plume in spring compared to autumn. Previous work has shown that algal blooms often occur in the frontal zone of plumes (Lv et al., 2022), which is consistent with our findings. In autumn, algal blooms (Chl-*a* > 10 μg L^{-1}) were observed throughout the water column in the offshore region of section CJ due to the water mixing caused by the typhoon. The enhanced growth of phytoplankton nearly depleted the DIN and PO_4-P concentrations (Figure 3). Typhoon-induced algal blooms in the offshore region of the CJ section produced large amounts of fresh organic matter. Previous work on 35 typhoon events during 2002–2011 showed that the depth-integrated primary productivity in the post-typhoon period increased by 19.7% and 12.2% in the coastal and continental shelf regions of ECS, respectively (Chen et al., 2017). These episodic events may also facilitate the intrusion of nutrient-rich Kuroshio subsurface water into the shelf, thereby supporting new production and generating bioavailable POM.

Low PAA-C% values (5−10%) were found in the YSCWM, TWC and YSCC influenced regions, indicating POM is of limited bioavailability. In the YSCWM-influenced region below 20 m of section 3300, PAA-C% values decreased sharply relative to the surface layer. Recent observations based on amino sugars also indicated a low bioreactivity of POM within the YSCWM (Guo, Shen, et al., 2023). Enhanced remineralization due to increased POM residence time in the water column induced by cyclonic eddies is considered a possible reason. Low PAA-C% values (<10%) found in the TWC-affected DH section were consistent with previous findings that TWC is characterized by low primary productivity and exhibits little seasonal variation (Gong et al., 2000; Liu et al., 2010). Although typhoons promote water mixing, the depleted nutrients of TWC limit the production of fresh phytoplankton organic matter. Similar results were reported by Guo et al. (2018) for labile dissolved organic matter concentrations using incubation experiments. In contrast, high nutrient concentrations but relatively low PAA-C% values (7−15%) were found in the nearshore zone of section CJ in autumn. Heterotrophic activity decomposes labile organic matter and is typically associated with a decrease in DO and the regeneration of nutrients. Depleted oxygen levels observed in the nearshore area of the CJ section in autumn coincided with lower PAA-C%, suggesting that POM had undergone extensive microbial alteration. This observation supports the notion that the high nutrients in this region were derived from local remineralization rather than CDW. High nutrient yet low Chl-*a* and low POM bioavailability were also found in the nearshore YSCC-influenced area of transect 3300. It appears that this distribution pattern is related to light limitation of phytoplankton growth as evidenced by the elevated total suspended matter concentrations (Figure S2 in Supporting Information S1). Taken together, these observations suggest that the primary production in the CEAA is largely controlled by hydrodynamically driven nutrient availability, thereby affecting POM distributions and bioavailability.

4.3. Biological Hot Spots and Implications for Carbon Sequestration

Labile organic matter can rapidly produce microbial responses resulting in a cascade of biogeochemical processes in specific regions, thereby creating biological hot spots (McClain et al., 2003; Shen et al., 2016; Stocker et al., 2008). Incubation experiments and field investigations have shown that the supply of bioactive substrates stimulates increases in bacterial biomass and production (Buchan et al., 2014; Lønborg et al., 2022; Obernosterer et al., 2008). Likewise, in the present study, we found that regions with elevated bioavailable POM were associated with heterotrophic bacterial blooms (significant positive correlations were found between PAA-C% and HBA; Figure S3 in Supporting Information S1; spring: $r = 0.40$, $p < 0.01$; autumn: $r = 0.61$, $p < 0.01$). Microbial communities may vary with the composition and reactivity of organic matter (Zhang et al., 2016; Zhou et al., 2021). To further investigate the bacterial response to POM bioactivity, we selected the 3300 section for bacterial community structure analysis. The results showed that high PAA-C% typically coincided with relatively high Bacteroidia abundance (Figure S1 in Supporting Information S1), indicating that fresh POM can rapidly stimulate the growth of Bacteroidia. Our findings are consistent with studies reporting that Bacteroidia are considered to be associated with the degradation of organic matter from phytoplankton (Fandino et al., 2001; Rink et al., 2007). In autumn, markedly high relative abundances (40−60%) of Oxyphotobacteria were found in the central and offshore surface layers of section 3300 (Figure S1 in Supporting Information S1). Oxyphotobacteria are photoautotrophic bacteria, and their production can contribute to bioavailable POM, suggesting that Oxyphotobacteria play an important role in the formation of biological hot spots.

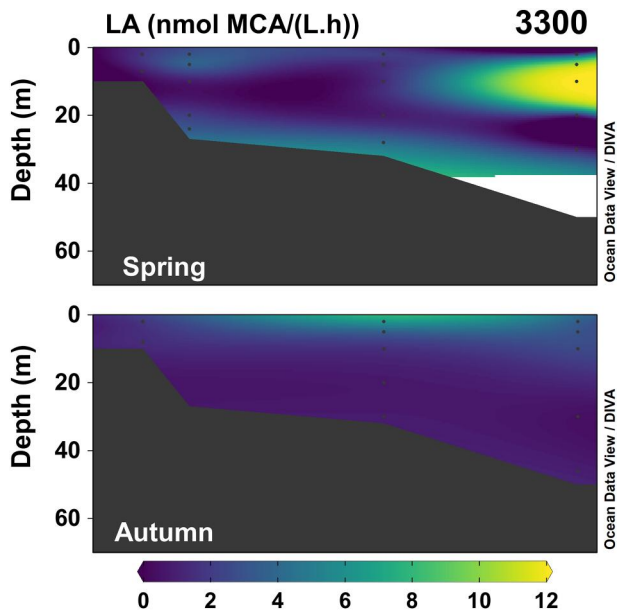

Figure 7. Vertical distributions of leucine aminopeptidases (LA) concentrations along section 3300 in the Changjiang Estuary and adjacent sea in spring and autumn.

Biological hot spots likely represent important sites for heterotrophic metabolism and carbon sequestration. Microbes require extracellular enzymatic hydrolysis for the uptake of organic macromolecules, since the cell membrane only allows transmembrane transport of molecules smaller than 600 Da (Weiss et al., 1991). Significant positive correlations were found between EEA and PAA-C% for both seasons (Figure 7; spring: $r = 0.49$, $p < 0.01$; autumn: $r = 0.67$, $p < 0.01$), indicating that bioavailable POM facilitates heterotrophic metabolism. Bacterial metabolism can convert labile organic matter to refractory organic matter, thus contributing to long-term carbon sequestration (Jiao et al., 2010). The bacterial growth efficiency (BGE) varies from 0.1 to 63 in coastal systems, but there is evidence of elevated BGE in nutrient-rich, highly productive waters (del Giorgio et al., 1997; Lønborg et al., 2022; Rivkin & Legendre, 2001). In the eutrophic CEAA, regions with high bacterial organic carbon contributions are associated with biological hot spots as indicated by the significant positive correlations between PAA-C% and bacterial contribution (Figure S4 in Supporting Information S1; spring: $r = 0.70$, $p < 0.01$; autumn: $r = 0.55$, $p < 0.01$), suggesting that hydrodynamically driven biological hot spots promote potential carbon sequestration (Zhu et al., 2014). Assuming a carbon content of 6.3 fg per bacterial cell (Kawasaki et al., 2011), we estimated the contribution of living heterotrophic bacteria to POC. Only ~1/3 of POC was found to be associated with intact bacterial cells, and a large portion (~2/3) of bacterial organic matter was present as bacterial detritus, which is consistent with previous findings (Kawasaki et al., 2011; Khodse & Bhosle, 2013; Ren et al., 2020). Despite a portion of the bacterial detritus being rapidly consumed, bacterial detritus is characterized by lower reactivity relative to intact cells. A high contribution of bacterial detritus implies that more bacterial organic carbon can enter the refractory carbon pool. These findings further support that heterotrophic metabolism largely drives carbon sequestration (Lechtenfeld et al., 2015).

Typhoon and cyclonic eddy-induced supply of nutrients results in the occurrence of patches with high phytoplankton production even in remote regions less affected by terrestrial inputs, appearing to enhance the sequestration efficiency of the biological carbon pump. Nevertheless, Zhou et al. (2020) suggested that the presence of cyclonic eddies did not increase carbon export, but rather served as a silica pump. In addition, typhoons promote CO_2 uptake by phytoplankton while also transporting CO_2-rich water from the deep to surface water, thereby potentially causing a net CO_2 transfer to the atmosphere (Li et al., 2019). As global warming and anthropogenic impacts intensify, biogeochemical processes involving organic matter in marginal seas become more intricate. Further studies are required to determine the net feedback effects of hydrodynamically driven biological hot spots on atmospheric CO_2 concentrations.

5. Conclusions

This study presents an integrated investigation of the physical, chemical, and biological properties of suspended POM in coastal waters under the influence of a large river. Our observations indicate that hydrodynamic processes such as river plumes, cyclonic eddies, and typhoons can contribute to the production of bioavailable POM by enhancing nutrient supply. Hot spots of elevated POM bioavailability represent sites of rapid bacterial transformation of labile POM into bacterial detritus, thus assisting carbon sequestration. Taken together, these new findings provide insights into the mechanisms of carbon cycling in marginal seas.

Data Availability Statement

The data presented in this study are archived at figshare.com and can be accessed via https://figshare.com/s/dbef22db0f7678c808a6 (Guo et al., 2024).

Acknowledgments
We thank the crew of the R/V *Kexue 3* for sampling assistance. Jinqiang Guo also thanks the China Scholarship Council (CSC), Deutscher Akademischer Austauschdienst (DAAD) and GEOMAR for additional support. This work was supported by the National Natural Science Foundation of China (Grant 42276038), Laoshan Laboratory (Grant LSKJ202204001), the Strategic Priority Research Program of the Chinese Academy of Sciences (Grant XDA23050501), the Shandong Provincial Natural Science Foundation (Grant ZR2020YQ28), the Taishan Scholars Program (Grant tsqn202211256), and the Two-Hundred Talents Plan of Yantai Scholar Project Special Funding.

References

Amon, R., & Benner, R. (1998). Seasonal patterns of bacterial abundance and production in the Mississippi River plume and their importance for the fate of enhanced primary production. *Microbial Ecology*, *35*(3), 289–300. https://doi.org/10.1007/s002489900084

Amon, R., Fitznar, H., & Benner, R. (2001). Linkages among the bioreactivity, chemical composition, and diagenetic state of marine dissolved organic matter. *Limnology & Oceanography*, *46*(2), 287–297. https://doi.org/10.4319/lo.2001.46.2.0287

Andersson, A., & Mackenzie, F. (2004). Shallow-water oceans: A source or sink of atmospheric CO_2? *Frontiers in Ecology and the Environment*, *2*(7), 348–353. https://doi.org/10.2307/3868359

Bao, R., van der Voort, T. S., Zhao, M., Guo, X., Montlucon, D. B., McIntyre, C., & Eglinton, T. I. (2018). Influence of hydrodynamic processes on the fate of sedimentary organic matter on continental margins. *Global Biogeochemical Cycles*, *32*(9), 1420–1432. https://doi.org/10.1029/2018GB005921

Bauer, J. E., Cai, W., Raymond, P. A., Bianchi, T. S., Hopkinson, C. S., & Regnier, P. A. G. (2013). The changing carbon cycle of the coastal ocean. *Nature*, *504*(7478), 61–70. https://doi.org/10.1038/nature12857

Borges, A., Delille, B., & Frankignoulle, M. (2005). Budgeting sinks and sources of CO_2 in the coastal ocean: Diversity of ecosystems counts. *Geophysical Research Letters*, *32*(14). https://doi.org/10.1029/2005GL023053

Bryan, J. R., Riley, J. P., & Williams, P. J. L. (1976). A Winkler procedure for making precise measurements of oxygen concentration for productivity and related studies. *Journal of Experimental Marine Biology and Ecology*, *21*(3), 191–197. https://doi.org/10.1016/0022-0981(76)90114-3

Buchan, A., LeCleir, G. R., Gulvik, C. A., & Gonzalez, J. M. (2014). Master recyclers: Features and functions of bacteria associated with phytoplankton blooms. *Nature Reviews Microbiology*, *12*(10), 686–698. https://doi.org/10.1038/nrmicro3326

Burdige, D. (2005). Burial of terrestrial organic matter in marine sediments: A re-assessment. *Global Biogeochemical Cycles*, *19*(4). https://doi.org/10.1029/2004GB002368

Cai, W. (2011). Estuarine and coastal ocean carbon paradox: CO_2 sinks or sites of terrestrial carbon incineration? *Annual Review of Marine Science*, *3*(1), 123–145. https://doi.org/10.1146/annurev-marine-120709-142723

Canuel, E. A., & Hardison, A. K. (2016). Sources, ages, and alteration of organic matter in estuaries. *Annual Review of Marine Science*, *8*(1), 409–434. https://doi.org/10.1146/annurev-marine-122414-034058

Chang, P., & Isobe, A. (2003). A numerical study on the Changjiang diluted water in the Yellow and East China Seas. *Journal of Geophysical Research*, *108*(C9), 1–17. https://doi.org/10.1029/2002JC001749

Chen, C. T. A. (2009). Chemical and physical fronts in the Bohai, Yellow and East China Seas. *Journal of Marine Systems*, *78*(3), 394–410. https://doi.org/10.1016/j.jmarsys.2008.11.016

Chen, D., He, L., Liu, F., & Yin, K. (2017). Effects of typhoon events on chlorophyll and carbon fixation in different regions of the East China Sea. *Estuarine, Coastal and Shelf Science*, *194*, 229–239. https://doi.org/10.1016/j.ecss.2017.06.026

Chen, Y., Wang, P., Shi, D., Ji, C., Chen, R., Gao, X., & Yang, G. (2021). Distribution and bioavailability of dissolved and particulate organic matter in different water masses of the Southern Yellow Sea and East China Sea. *Journal of Marine Systems*, *222*, 103596. https://doi.org/10.1016/j.jmarsys.2021.103596

Cowie, G., & Hedges, J. (1994). Biochemical indicators of diagenetic alteration in natural organic-matter mixtures. *Nature*, *369*(6478), 304–307. https://doi.org/10.1038/369304a0

Dai, M., Cao, Z., Guo, X., Zhai, W., Liu, Z., Yin, Z., et al. (2013). Why are some marginal seas sources of atmospheric CO_2? *Geophysical Research Letters*, *40*(10), 2154–2158. https://doi.org/10.1002/grl.50390

Dai, M., Su, J., Zhao, Y., Hofmann, E. E., Cao, Z., Cai, W.-J., et al. (2022). Carbon fluxes in the coastal ocean: Synthesis, boundary processes, and future trends. *Annual Review of Earth and Planetary Sciences*, *50*(1), 593–626. https://doi.org/10.1146/annurev-earth-032320-090746

Dauwe, B., Middelburg, J., Herman, P., & Heip, C. (1999). Linking diagenetic alteration of amino acids and bulk organic matter reactivity. *Limnology & Oceanography*, *44*(7), 1809–1814. https://doi.org/10.4319/lo.1999.44.7.1809

Davis, J., & Benner, R. (2005). Seasonal trends in the abundance, composition and bioavailability of particulate and dissolved organic matter in the Chukchi/Beaufort Seas and western Canada Basin. *Deep Sea Research Part II: Topical Studies in Oceanography*, *52*(24–26), 3396–3410. https://doi.org/10.1016/j.dsr2.2005.09.006

Davis, J., Kaiser, K., & Benner, R. (2009). Amino acid and amino sugar yields and compositions as indicators of dissolved organic matter diagenesis. *Organic Geochemistry*, *40*(3), 343–352. https://doi.org/10.1016/j.orggeochem.2008.12.003

del Giorgio, P., Cole, J., & Cimbleris, A. (1997). Respiration rates in bacteria exceed phytoplankton production in unproductive aquatic systems. *Nature*, *385*(6612), 148–151. https://doi.org/10.1038/385148a0

Dittmar, T., Fitznar, H., & Kattner, G. (2001). Origin and biogeochemical cycling of organic nitrogen in the eastern Arctic Ocean as evident from D- and L-amino acids. *Geochimica et Cosmochimica Acta*, *65*(22), 4103–4114. https://doi.org/10.1016/S0016-7037(01)00688-3

Fandino, L., Riemann, L., Steward, G., Long, R., & Azam, F. (2001). Variations in bacterial community structure during a dinoflagellate bloom analyzed by DGGE and 16S rDNA sequencing. *Aquatic Microbial Ecology*, *23*(2), 119–130. https://doi.org/10.3354/ame023119

Fitznar, H., Lobbes, J., & Kattner, G. (1999). Determination of enantiomeric amino acids with high-performance liquid chromatography and pre-column derivatisation with o-phthaldialdehyde and N-isobutyrylcysteine in seawater and fossil samples (mollusks). *Journal of Chromatography A*, *832*(1–2), 123–132. https://doi.org/10.1016/S0021-9673(98)01000-0

Gattuso, J., Frankignoulle, M., & Wollast, R. (1998). Carbon and carbonate metabolism in coastal aquatic ecosystems. *Annual Review of Ecology and Systematics*, *29*(1), 405–434. https://doi.org/10.1146/annurev.ecolsys.29.1.405

Gong, G., Shiah, F., Liu, K., Wen, Y., & Liang, M. (2000). Spatial and temporal variation of chlorophyll a, primary productivity and chemical hydrography in the southern East China Sea. *Continental Shelf Research*, *20*(4–5), 411–436. https://doi.org/10.1016/S0278-4343(99)00079-5

Guo, J., Liang, S., Li, X., Li, W., Wang, Y., & Su, R. (2018). Composition and bioavailability of dissolved organic matter in different water masses of the East China Sea. *Estuarine, Coastal and Shelf Science*, *212*, 189–202. https://doi.org/10.1016/j.ecss.2018.07.009

Guo, J., Shen, Y., Yuan, H., Song, J., Li, X., Duan, L., & Li, N. (2023). Bacterial reworking of particulate organic matter in a dynamic marginal sea: Implications for carbon sequestration. *Organic Geochemistry*, *179*, 104583. https://doi.org/10.1016/j.orggeochem.2023.104583

Guo, J., Yuan, H., Song, J., Li, X., & Duan, L. (2020). Hypoxia, acidification and nutrient accumulation in the Yellow Sea Cold Water of the South Yellow Sea. *Science of the Total Environment*, *745*, 141050. https://doi.org/10.1016/j.scitotenv.2020.141050

Guo, J., Zhou, B., Achterberg, E. P., Song, J., Duan, L., Li, X., & Yuan, H. (2024). Influence of hydrodynamics on the composition and reactivity of particulate organic matter in a large river influenced ocean margin (Version 2) [Dataset]. Figshare. https://doi.org/10.6084/m9.figshare.23968077.v2

Guo, J., Zhou, B., Achterberg, E. P., Yuan, H., Song, J., Duan, L., & Li, X. (2023). Rapid cycling of bacterial particulate organic matter in the upper layer of the Western Pacific Warm Pool. *Geophysical Research Letters*, *50*(11). https://doi.org/10.1029/2023GL102896

Guo, S., Feng, Y., Wang, L., Dai, M., Liu, Z., Bai, Y., & Sun, J. (2014). Seasonal variation in the phytoplankton community of a continental-shelf sea: The East China sea. *Marine Ecology Progress Series*, *516*, 103–126. https://doi.org/10.3354/meps10952

Herndl, G. J., & Reinthaler, T. (2013). Microbial control of the dark end of the biological pump. *Nature Geoscience*, *6*(9), 718–724. https://doi.org/10.1038/NGEO1921

Hoppe, H. G. (1993). Use of fluorogenic model substrates for extracellular enzyme activity (EEA) measurement of bacteria. In P. F. Kemp, J. J. Cole, B. F. Sherr, & E. B. Sherr (Eds.), *Handbook of methods in aquatic microbial ecology* (pp. 423–431). Lewis Publishers. https://doi.org/10.1201/9780203752746

Hu, J., & Wang, X. H. (2016). Progress on upwelling studies in the China seas. *Reviews of Geophysics*, *54*(3), 653–673. https://doi.org/10.1002/2015RG000505

Isobe, A., Ando, M., Watanabe, T., Senjyu, T., Sugihara, S., & Manda, A. (2002). Freshwater and temperature transports through the Tsushima-Korea Straits. *Journal of Geophysical Research*, *107*(C7). https://doi.org/10.1029/2000JC000702

Jiao, N., Herndl, G. J., Hansell, D. A., Benner, R., Kattner, G., Wilhelm, S. W., et al. (2010). Microbial production of recalcitrant dissolved organic matter: Long-term carbon storage in the global ocean. *Nature Reviews Microbiology*, *8*(8), 593–599. https://doi.org/10.1038/nrmicro2386

Kaiser, K., & Benner, R. (2005). Hydrolysis-induced racemization of amino acids. *Limnology and Oceanography: Methods*, *3*(8), 318–325. https://doi.org/10.4319/lom.2005.3.318

Kaiser, K., & Benner, R. (2008). Major bacterial contribution to the ocean reservoir of detrital organic carbon and nitrogen. *Limnology & Oceanography*, *53*(3), 99–112. https://doi.org/10.4319/lo.2008.53.1.0099

Kaiser, K., & Benner, R. (2012). Organic matter transformations in the upper mesopelagic zone of the North Pacific: Chemical composition and linkages to microbial community structure. *Journal of Geophysical Research*, *117*(C1). https://doi.org/10.1029/2011JC007141

Kawasaki, N., Sohrin, R., Ogawa, H., Nagata, T., & Benner, R. (2011). Bacterial carbon content and the living and detrital bacterial contributions to suspended particulate organic carbon in the North Pacific Ocean. *Aquatic Microbial Ecology*, *62*(2), 165–176. https://doi.org/10.3354/ame01462

Kellogg, C. T., & Deming, J. W. (2014). Particle-associated extracellular enzyme activity and bacterial community composition across the Canadian Arctic Ocean. *FEMS Microbiology Ecology*, *89*(2), 360–375. https://doi.org/10.1111/1574-6941.12330

Khodse, V. B., & Bhosle, N. B. (2013). Distribution, origin and transformation of amino sugars and bacterial contribution to estuarine particulate organic matter. *Continental Shelf Research*, *68*, 33–42. https://doi.org/10.1016/j.csr.2013.08.004

Lan, J., Wang, Y., & Wang, G. (2010). A subsurface intensity index of the cold eddy in the East China Sea. *Chinese Journal of Oceanology and Limnology*, *28*(6), 1275–1280. https://doi.org/10.1007/s00343-010-9015-4

Lechtenfeld, O. J., Hertkorn, N., Shen, Y., Witt, M., & Benner, R. (2015). Marine sequestration of carbon in bacterial metabolites. *Nature Communications*, *6*(1), 6711. https://doi.org/10.1038/ncomms7711

Lee, S., & Beardsley, R. (1999). Influence of stratification on residual tidal currents in the Yellow Sea. *Journal of Geophysical Research*, *104*(C7), 15679–15701. https://doi.org/10.1029/1999JC900108

Lehmann, M. F., Carstens, D., Deek, A., McCarthy, M., Schubert, C. J., & Zopfi, J. (2020). Amino acid and amino sugar compositional changes during in vitro degradation of algal organic matter indicate rapid bacterial re-synthesis. *Geochimica et Cosmochimica Acta*, *283*, 67–84. https://doi.org/10.1016/j.gca.2020.05.025

Li, D., Chen, J., Ni, X., Wang, K., Zeng, D., Wang, B., et al. (2019). Hypoxic bottom waters as a carbon source to atmosphere during a typhoon passage over the East China Sea. *Geophysical Research Letters*, *46*(20), 11329–11337. https://doi.org/10.1029/2019GL083933

Li, H., Tang, H., Shi, X., Zhang, C., & Wang, X. (2014). Increased nutrient loads from the Changjiang (Yangtze) River have led to increased harmful algal blooms. *Harmful Algae*, *39*, 92–101. https://doi.org/10.1016/j.hal.2014.07.002

Li, X., Liu, Z., Chen, W., Wang, L., He, B., Wu, K., et al. (2018). Production and transformation of dissolved and particulate organic matter as indicated by amino acids in the Pearl River Estuary, China. *Journal of Geophysical Research: Biogeosciences*, *123*(12), 3523–3537. https://doi.org/10.1029/2018JG004690

Liang, S., Li, S., Guo, J., Yang, Y., Xu, Z., Zhang, M., et al. (2023). Source, composition, and reactivity of particulate organic matter along the Changjiang Estuary salinity gradient and adjacent sea. *Marine Chemistry*, *252*, 104245. https://doi.org/10.1016/j.marchem.2023.104245

Liu, K. K., Chao, S. Y., Lee, H. J., Gong, G. C., & Teng, Y. C. (2010). Seasonal variation of primary productivity in the East China Sea: A numerical study based on coupled physical-biogeochemical model. *Deep Sea Research Part II: Topical Studies in Oceanography*, *57*(19–20), 1762–1782. https://doi.org/10.1016/j.dsr2.2010.04.003

Liu, Q., Kandasamy, S., Wang, H., Wang, L., Lin, B., Gao, A., & Chen, C.-T. A. (2019). Impact of hydrological conditions on the biogeochemical dynamics of suspended particulate organic matter in the upper mixed layer of the Southern East China Sea. *Journal of Geophysical Research: Oceans*, *124*(8), 6120–6140. https://doi.org/10.1029/2019JC015193

Lønborg, C., Baltar, F., Calleja, M. L. I., & Morán, X. A. G. (2022). Heterotrophic bacteria respond differently to increasing temperature and dissolved organic carbon sources in two tropical coastal systems. *Journal of Geophysical Research: Biogeosciences*, *127*(12), e2022JG006890. https://doi.org/10.1029/2022JG006890

Lv, T., Liu, D., Zhou, P., Lin, L., Wang, Y., & Wang, Y. (2022). The coastal front modulates the timing and magnitude of spring phytoplankton bloom in the Yellow Sea. *Water Research*, *220*, 118669. https://doi.org/10.1016/j.watres.2022.118669

McCarthy, M., Hedges, J., & Benner, R. (1998). Major bacterial contribution to marine dissolved organic nitrogen. *Science*, *281*(5374), 231–234. https://doi.org/10.1126/science.281.5374.231

McClain, M., Boyer, E., Dent, C., Gergel, S., Grimm, N., Groffman, P., et al. (2003). Biogeochemical hot spots and hot moments at the interface of terrestrial and aquatic ecosystems. *Ecosystems*, *6*(4), 301–312. https://doi.org/10.1007/s10021-003-0161-9

Obernosterer, I., Christaki, U., Lefèvre, D., Catala, P., Van Wambeke, F., & Lebaron, P. (2008). Rapid bacterial mineralization of organic carbon produced during a phytoplankton bloom induced by natural iron fertilization in the Southern Ocean. *Deep Sea Research Part II: Topical Studies in Oceanography*, *55*(5–7), 777–789. https://doi.org/10.1016/j.dsr2.2007.12.005

Pedrosa-Pamies, R., Sanchez-Vidal, A., Calafat, A., Canals, M., & Duran, R. (2013). Impact of storm-induced remobilization on grain size distribution and organic carbon content in sediments from the Blanes Canyon area, NW Mediterranean Sea. *Progress in Oceanography*, *118*(SI), 122–136. https://doi.org/10.1016/j.pocean.2013.07.023

Ren, C., Yuan, H., Song, J., Duan, L., Li, X., Li, N., & Zhou, B. (2020). The use of amino sugars for assessing seasonal dynamics of particulate organic matter in the Yangtze River estuary. *Marine Chemistry*, *220*, 103763. https://doi.org/10.1016/j.marchem.2020.103763

Rink, B., Seeberger, S., Martens, T., Duerselen, C.-D., Simon, M., & Brinkhoff, T. (2007). Effects of phytoplankton bloom in a coastal ecosystem on the composition of bacterial communities. *Aquatic Microbial Ecology*, *48*(1), 47–60. https://doi.org/10.3354/ame048047

Rivkin, R., & Legendre, L. (2001). Biogenic carbon cycling in the upper ocean: Effects of microbial respiration. *Science*, *291*(5512), 2398–2400. https://doi.org/10.1126/science.291.5512.2398

Shen, Y., Benner, R., Murray, A. E., Gimpel, C., Mitchell, B. G., Weiss, E. L., & Reiss, C. (2017). Bioavailable dissolved organic matter and biological hot spots during austral winter in Antarctic waters. *Journal of Geophysical Research: Oceans*, *122*(1), 508–520. https://doi.org/10.1002/2016JC012301

Shen, Y., Fichot, C. G., Liang, S. K., & Benner, R. (2016). Biological hot spots and the accumulation of marine dissolved organic matter in a highly productive ocean margin. *Limnology & Oceanography*, *61*(4), 1287–1300. https://doi.org/10.1002/lno.10290

Shi, F., Luo, Y., & Rong, Z. (2016). A numerical study of the summer circulation in the southwestern Yellow Sea. *Acta Oceanologica Sinica*, *35*(11), 1–8. https://doi.org/10.1007/s13131-016-0943-5

Shih, Y. Y., Hung, C. C., Tuo, S. H., Shao, H. J., Chow, C. H., Muller, F. L. L., & Cai, Y. H. (2020). The impact of eddies on nutrient supply, diatom biomass and carbon export in the northern South China Sea. *Frontiers in Earth Science*, *8*. https://doi.org/10.3389/feart.2020.537332

Siswanto, E., Morimoto, A., & Kojima, S. (2009). Enhancement of phytoplankton primary productivity in the southern East China Sea following episodic typhoon passage. *Geophysical Research Letters*, *36*(11). https://doi.org/10.1029/2009GL037883

Stocker, R., Seymour, J. R., Samadani, A., Hunt, D. E., & Polz, M. F. (2008). Rapid chemotactic response enables marine bacteria to exploit ephemeral microscale nutrient patches. *Proceedings of the National Academy of Sciences of the United States of America*, *105*(11), 4209–4214. https://doi.org/10.1073/pnas.0709765105

Unger, D., Ittekkot, V., Schafer, P., & Tiemann, J. (2005). Biogeochemistry of particulate organic matter from the Bay of Bengal as discernible from hydrolysable neutral carbohydrates and amino acids. *Marine Chemistry*, *96*(1–2), 155–184. https://doi.org/10.1016/j.marchem.2004.12.005

Wang, B., Hirose, N., Kang, B., & Takayama, K. (2014). Seasonal migration of the Yellow Sea Bottom Cold Water. *Journal of Geophysical Research: Oceans*, *119*(7), 4430–4443. https://doi.org/10.1002/2014JC009873

Wei, Q., Yao, P., Xu, B., Zhao, B., Ran, X., Zhao, Y., et al. (2021). Coastal upwelling combined with the river plume regulates hypoxia in the Changjiang Estuary and adjacent inner East China Sea shelf. *Journal of Geophysical Research: Oceans*, *126*(11). https://doi.org/10.1029/2021JC017740

Weiss, M., Abele, U., Weckesser, J., Welte, W., Schiltz, E., & Schulz, G. (1991). Molecular architecture and electrostatic properties of a bacterial porin. *Science*, *254*(5038), 1627–1630. https://doi.org/10.1126/science.1721242

Wu, Y., Dittmar, T., Ludwichowski, K., Kattner, G., Zhang, J., Zhu, Z., & Koch, B. (2007). Tracing suspended organic nitrogen from the Yangtze river catchment into the East China Sea. *Marine Chemistry*, *107*(3), 367–377. https://doi.org/10.1016/j.marchem.2007.01.022

Yang, D., Yin, B., Liu, Z., & Feng, X. (2011). Numerical study of the ocean circulation on the East China Sea shelf and a Kuroshio bottom branch northeast of Taiwan in summer. *Journal of Geophysical Research*, *116*(C5), C05015. https://doi.org/10.1029/2010JC006777

Zhang, J., Liu, S. M., Ren, J. L., Wu, Y., & Zhang, G. L. (2007). Nutrient gradients from the eutrophic Changjiang (Yangtze River) estuary to the oligotrophic Kuroshio waters and re-evaluation of budgets for the East China Sea Shelf. *Progress in Oceanography*, *74*(4), 449–478. https://doi.org/10.1016/j.pocean.2007.04.019

Zhang, Y., Xiao, W., & Jiao, N. (2016). Linking biochemical properties of particles to particle-attached and free-living bacterial community structure along the particle density gradient from freshwater to open ocean. *Journal of Geophysical Research: Biogeosciences*, *121*(8), 2261–2274. https://doi.org/10.1002/2016JG003390

Zhao, Y., Li, Z., Tian, X., Sanjun, Z., Jiliang, X., Chaolun, L., & Xiouren, N. (2011). Spatial and temporal variation of picoplankton distribution in the Yellow Sea, China. *Chinese Journal of Oceanology and Limnology*, *29*(1), 150–161. https://doi.org/10.1007/s00343-011-9086-x

Zhou, B., Yuan, H., Song, J., Li, X., Li, N., Duan, L., & Yu, L. (2021). Source, transformation and degradation of particulate organic matter and its connection to microbial processes in Jiaozhou Bay, North China. *Estuarine, Coastal and Shelf Science*, *260*, 107501. https://doi.org/10.1016/j.ecss.2021.107501

Zhou, K., Dai, M., Xiu, P., Wang, L., Hu, J., & Benitez-Nelson, C. R. (2020). Transient enhancement and decoupling of carbon and opal export in cyclonic eddies. *Journal of Geophysical Research: Oceans*, *125*(9). https://doi.org/10.1029/2020JC016372

Zhu, Z., Zhang, J., Wu, Y., Zhang, Y., Lin, J., & Liu, S. (2011). Hypoxia off the Changjiang (Yangtze River) Estuary: Oxygen depletion and organic matter decomposition. *Marine Chemistry*, *125*(1–4), 108–116. https://doi.org/10.1016/j.marchem.2011.03.005

Zhu, Z. Y., Wu, Y., Zhang, J., Dittmar, T., Li, Y., Shao, L., & Ji, Q. (2014). Can primary production contribute non-labile organic matter in the sea: Amino acid enantiomers along the coast south of the Changjiang Estuary in May. *Journal of Marine Systems*, *129*, 343–349. https://doi.org/10.1016/j.jmarsys.2013.07.018

Zhu, Z. Y., Zhang, J., Wu, Y., & Lin, J. (2006). Bulk particulate organic carbon in the East China Sea: Tidal influence and bottom transport. *Progress in Oceanography*, *69*(1), 37–60. https://doi.org/10.1016/j.pocean.2006.02.014